

This discussion paper is/has been under review for the journal Atmospheric Chemistry and Physics (ACP). Please refer to the corresponding final paper in ACP if available.

**Biomass burning
plume heights using
aerosol index
measurements**

H. Guan et al.

A multi-decadal history of biomass burning plume heights identified using aerosol index measurements

H. Guan^{1,2}, R. Esswein^{1,2}, J. Lopez^{1,2}, R. Bergstrom^{1,2}, A. Warnock³,
M. Follette-Cook^{4,*}, M. Fromm⁴, and L. Iraci²

¹Bay Area Environmental Research Institute, Sonoma, CA, USA

²NASA Ames Research Center, Moffett Field, CA, USA

³University of Michigan, Ann Arbor, MI, USA

⁴Remote Sensing Division, Naval Research Laboratory, Washington DC, USA

* currently at: Goddard Earth Sciences and Technology Center, University of Maryland Baltimore County, Baltimore, MD, USA

Received: 14 November 2009 – Accepted: 15 December 2009 – Published: 5 January 2010

Correspondence to: H. Guan (hong.guan-1@nasa.gov)

Published by Copernicus Publications on behalf of the European Geosciences Union.

Title Page

Abstract

Introduction

Conclusions

References

Tables

Figures

⏪

⏩

◀

▶

Back

Close

Full Screen / Esc

Printer-friendly Version

Interactive Discussion

Abstract

We have quantified the relationship between Aerosol Index (AI) measurements and plume height for young biomass burning plumes using coincident OMI and CALIPSO measurements. This linear relationship allows the determination of high-altitude plumes wherever AI data are available, and it provides a data set for validating global fire plume injection heights in chemistry transport models. We find that all plumes detected from June 2006 to February 2009 with an AI value ≥ 9 are located at altitudes higher than 5 km. Older high-altitude plumes have lower AI values than young plumes at similar altitudes. We have examined available AI data from the OMI and TOMS instruments (1978–2009) and find that large AI plumes occur more frequently over North America than over Australia or Russia/Northeast Asia. According to the derived relationship, during this time interval, 181 plumes reached altitudes above 8 km. One hundred and thirty-two had injection heights ≥ 8 km but below 12 km, and 49 were lofted to 12 km or higher, including 14 plumes injected above 16 km.

1 Introduction

Knowledge of the injection and transport altitudes of biomass burning plumes is crucial for understanding the long range transport of particles and reactive gases that can substantially alter the radiation balance and chemistry of the atmosphere (Luderer et al., 2006; Trentmann et al., 2006; Cofer et al., 1996; Waibel et al., 1999; Jost et al., 2004; Forster et al., 2001; IPCC, 2007; Randerson et al., 2006; Jeong and Hsu, 2008). Remote and in-situ observations have documented many instances of biomass burning pollutants in the upper troposphere and lower stratosphere (UT/LS) (Fromm and Servranckx, 2003; Rosenfeld et al., 2007; Jost et al., 2004).

To date, biomass burning plume heights have typically been determined in a case-by-case manner. For instance, using Polar Ozone and Aerosol Measurement III (POAM III) observations and back trajectories (Fromm et al., 2008a,b; Rosenfeld et al., 2007),

Biomass burning plume heights using aerosol index measurements

H. Guan et al.

Title Page

Abstract

Introduction

Conclusions

References

Tables

Figures

⏪

⏩

◀

▶

Back

Close

Full Screen / Esc

Printer-friendly Version

Interactive Discussion



**Biomass burning
plume heights using
aerosol index
measurements**

H. Guan et al.

[Title Page](#)[Abstract](#)[Introduction](#)[Conclusions](#)[References](#)[Tables](#)[Figures](#)[⏪](#)[⏩](#)[◀](#)[▶](#)[Back](#)[Close](#)[Full Screen / Esc](#)[Printer-friendly Version](#)[Interactive Discussion](#)

the May 2001 Chisholm fire in Alberta, Canada was determined to have penetrated the tropopause. In that study, over 200 observations of aerosol layers were measured by the POAM III mission, half of which were in the stratosphere. Another case study involved detection of high CO values 2 km above the tropopause south of Florida during an aircraft campaign in July of 2002 (Jost et al., 2004). Particle measurements by the Particle Analysis by Laser Mass Spectrometry (PALMS) instrument helped corroborate the biomass burning signature. In addition, isentropic back trajectories placed the air mass under a POAM III enhanced aerosol feature over Canada, showing evidence of stratospheric transport far from the observation location.

Mazzoni et al. (2007) used Multiangle Imaging SpectroRadiometer (MISR) and Moderate Resolution Imaging Spectroradiometer (MODIS) data to locate fires and their associated smoke plumes and retrieved the injection heights over a four-month period. They found a total of 325 candidate plumes, of which 138 were identified as biomass burning plumes, none of which were classified as stratospheric. Kahn et al. (2008) further assessed smoke injection height for a similar region and period. They noted that at least about 10% of wildfire smoke plumes reached the free troposphere but remained lower than 5 km. This low-altitude bias may be inherent in their selection criteria, as their plume observations are limited to the overpass time (11:00–14:00 LT in the North America region, Val Martin et al., 2009) of the Terra satellite, when fires have not yet reached their maximum intensity.

Val Martin et al. (2009) extended the work of Mazzoni et al. (2007) by analyzing a 5-yr record of MISR smoke plume heights over North America and correlating them with MODIS fire radiative power measurements. That study highlighted a physical relationship which could be explored to estimate injection heights for low-altitude fire plumes (lower than 7 km).

Recently, Jeong and Hsu (2008) presented a new algorithm that predicts the height of smoke aerosols associated with biomass burning when Aerosol Index (AI), single scattering albedo (SSA), and optical depth are known. They showed that for a specific biomass burning plume over the northwest United States (15 August 2007), the

predicted height and the Cloud-Aerosol Lidar and Infrared Pathfinder Satellite Observations (CALIPSO) measured height are in relatively good agreement. Their results showed that satellite data can be exploited in studies of larger scope.

5 Several models have been used to assess the impact of biomass burning pollution on the stratosphere (e.g., Luderer et al., 2006; Trentmann et al., 2006), the UT/LS (e.g., Duncan, 2007) and the troposphere (e.g., Kuester et al., 2005; Li et al., 2005). The injection height of smoke plumes from forest fires is a key input for aerosol transport modeling, as the height is critical for determining the distance and direction the smoke will travel (Colarco et al., 2004; Ginoux et al., 2001; Westphal and Toon, 1991).
10 However, the injection height is a large source of uncertainty in these models. Recently, efforts have been made to apply more realistic injection heights in chemistry transport models. These physically-based (Freitas et al., 2007; Guan et al., 2008) or MISR-derived (Chen et al., 2009) injection heights have only been validated in certain regions and for limited periods. In order to minimize uncertainties and limitations, it is
15 important to use a database of seasonally and regionally diverse injections, rather than simply compare model results to a handful of case studies.

We have developed a simple empirical method to identify biomass burning plume injection heights. AI is an ideal candidate for this task since it is sensitive to high-altitude aerosols and has a multi-decadal historical data set. We have used plume altitudes
20 measured from the CALIPSO instrument to develop a method for screening the entire AI data record for high altitude plumes. Using the relationship developed when altitude measurements are available, we screened the entire AI record and assembled a climatology of high-altitude biomass burning plumes from 1978 to 2009. In addition to providing a long-term, global data set for model validation, our data set also reveals
25 the patterns and numbers of high altitude biomass burning plumes in several regions worldwide.

**Biomass burning
plume heights using
aerosol index
measurements**

H. Guan et al.

Title Page

Abstract

Introduction

Conclusions

References

Tables

Figures



Back

Close

Full Screen / Esc

Printer-friendly Version

Interactive Discussion

2 Satellite data sets

2.1 Aerosol Index data

The AI is a measure of how backscattered ultraviolet (UV) radiation from an atmosphere containing aerosols differs from that of a pure molecular atmosphere¹. AI is especially sensitive to the presence of UV absorbing aerosols such as smoke, mineral dust, and volcanic ash. The index value is positive when absorbing aerosols are present, whereas clouds yield a nearly zero value of AI. Torres et al. (1998) and Jeong and Hsu (2008) showed that AI varies with aerosol layer height, optical depth and single scattering albedo. High and optically-thick absorbing aerosol layers more effectively reduce the scattered light from the Rayleigh scattering below the aerosol layer. In cloud-free conditions, the highest and thickest absorbing aerosols give the largest AI values. Absorbing aerosols can still be detected if mixed with clouds or located above clouds.

The Total Ozone Mapping Spectrometer (TOMS) instruments onboard the Nimbus 7 (1978–1993) and Earth Probe (1996–2005) satellites and the Ozone Monitoring Instrument (OMI) onboard the EOS-Aura (2004–present) satellite provide a nearly continuous and long term record of AI suitable for scientific applications. Daily TOMS version 8 Level 3 (1.25° × 1° resolution) and OMI Collection 3 (1° × 1° resolution) were obtained from the NASA/GSFC TOMS website (<http://toms.gsfc.nasa.gov/aerosols/>)

¹AI is defined as: $AI(\tau, \omega, z) = 100 (\log_{10}(I_{360\text{meas}}/I_{331\text{meas}}) - \log_{10}(I_{360\text{calc}}(R_{\text{sfc}})/I_{331\text{calc}}(R_{\text{sfc}})))$, where I is the radiance (or intensity) measured by the satellite or calculated for a purely molecular scattering atmosphere, and R_{sfc} is the Lambert Equivalent effective reflectivity value. This rather awkward definition is due to the origin of AI as a residual from satellite measurements (the term was called an “ N -valued residual” in the original Herman et al. (1997) paper. In practice the equation reduces to the negative of 100 times the log base 10 of the ratio of the measured radiance at a wavelength divided by the radiance that would be observed if the atmosphere had only molecular scattering. The use of AI has been discussed in a number of papers (Torres et al., 1998; Jeong and Hsu, 2008).

Biomass burning plume heights using aerosol index measurements

H. Guan et al.

Title Page

Abstract

Introduction

Conclusions

References

Tables

Figures

⏪

⏩

◀

▶

Back

Close

Full Screen / Esc

Printer-friendly Version

Interactive Discussion

aerosols.html, updated June 2009). TOMS AI data was unavailable between May 1993 and September 1996. Additionally, the EP-TOMS AI data after July 2000 were not included in this study due to the calibration drift of the sensor (Kiss et al., 2007).

Over bright clouds, AI values are enhanced due to the effect of the radiative transfer interactions between the bright underlying cloud and the absorbing layer (Hsu et al., 2004; Torres et al., 2007) and do not represent actual differences in aerosol physical properties. To avoid the enhanced effect of underlying clouds on AI, we screened out cloudy pixels that contained a cloud fraction (for OMI) or a reflectivity (for TOMS) of greater than 0.2 (personal communication, O. Torres, 2008).

2.2 CALIPSO data

CALIPSO's lidar instrument, the Cloud-Aerosol Lidar with Orthogonal Polarization (CALIOP), provides high resolution vertical profiles of aerosol and cloud attenuated backscatter signals at 532 nm and 1064 nm (Winker et al., 2007). The footprint of the lidar beam has a 100 m cross-section (Thomason et al., 2007). CALIPSO gives limited coverage relative to OMI (swath=2600 km) (Eckhardt et al., 2008).

Several products derived from the backscatter signals were used in this study. They included the version 2 Vertical Feature Mask (VFM) (Vaughan et al., 2004), the 532 nm total attenuated backscatter, the depolarization ratio (the ratio of the perpendicular component of the backscatter to the total backscatter), and the color ratio (the ratio of backscatter at 1064 nm to 532 nm). We used the VFM product to determine the top heights of features and then further distinguished the aerosol from cloud by checking 532 nm total attenuated backscatter, depolarization ratio, and color ratio. Details on distinguishing aerosols from clouds are described in Sect. 3.

Biomass burning plume heights using aerosol index measurements

H. Guan et al.

Title Page

Abstract

Introduction

Conclusions

References

Tables

Figures

⏪

⏩

◀

▶

Back

Close

Full Screen / Esc

Printer-friendly Version

Interactive Discussion

2.3 MODIS fire data

Additionally, MODIS fire count maps were used to detect the location and time of fires for the 2004–2009 period. Fire count data are available online at <http://firefly.geog.umd.edu/firemap/>.

3 Identification methodology for high-altitude plumes

We first used the AI data product to locate large aerosol plumes, defined as containing at least 1 pixel with $AI \geq 7$ and at least 2 (TOMS) or 3 (OMI) adjacent pixels with $AI \geq 4$. We found 1479 plumes over the AI record period (1978–2009, see Sect. 2.1 for specific dates). From that set, large AI observations caused by solar eclipses and volcanoes were removed. Major desert regions which are likely influenced by dust rather than smoke, such as North Africa and the Middle East, were excluded. Because the dust storm season overlaps with the wildfire season in Russia, Mongolia, and Northeast China, we screened out potential dust cases over the downwind regions of the Gobi and Taklamakan Deserts during spring by checking the MODIS fire product for the time period that a plume was first observable or by tracking the plume's geographical origin. In addition, news reports and published literature were used as tools in linking an aerosol plume to a dust signal, which were then removed from further analysis. We found 107 AI plumes likely due to smoke aerosol during the CALIPSO era (1 June 2006 to 13 February 2009). The location of these smoke plumes is displayed in Fig. 1.

Once smoke plumes were located, we determined the plume altitude following the steps highlighted in the flowchart of Fig. 2. We first used the CALIPSO level 2 VFM data to find the plume altitude. If the CALIPSO day track passed through the AI plume, we found the highest CALIPSO signal height inside the AI plume area. In cases where more than one CALIPSO track intersected the plume, the track that was closest to the location of the largest AI value was used. The highest-altitude signal observed by

Biomass burning plume heights using aerosol index measurements

H. Guan et al.

Title Page

Abstract

Introduction

Conclusions

References

Tables

Figures

⏪

⏩

◀

▶

Back

Close

Full Screen / Esc

Printer-friendly Version

Interactive Discussion

CALIPSO at the location of a large AI observation should be related only to absorbing aerosol, because cloud produces a near-zero AI value.

Because the AI grid may contain sub-pixel clouds, which can be explicitly detected by the high-resolution CALIPSO measurement, we also checked the available 532-nm total attenuated backscatter, CALIPSO depolarization ratio, and the color ratio images for each case to validate that the high-altitude signals did represent smoke aerosols. Unlike clouds, thin smoke plumes have a weak 532 nm total attenuated backscatter signal; however dense plumes may have a 532 nm backscatter signal similar to clouds. We distinguished dense smoke from cloud by checking for an obvious increase of color ratio with layer penetration depth coupled with low depolarization ratio (dominated by a value less than ~ 0.2) (personal communication, A. Omar, 2008). If the top signal was a cloud, we assigned the highest smoke-plume height within the plume track as the top height. The height uncertainty resulting from this manual assignment was approximately ± 0.5 km. Using the above method, we found 23 cases of coincident AI and CALIPSO measurements which are plotted in Fig. 3 and also denoted by orange symbols in Fig. 1.

By running a back trajectory model starting at each of the 23 AI plume locations and their associated maximum CALIPSO plume height, we linked each AI plume to the corresponding fire source region observed by MODIS and estimated the plume age. The trajectory model employed here was the Goddard kinematic trajectory model (Schoeberl and Newman, 1995) using National Centers for Environmental Prediction (NCEP) winds updated every 6 h on a $2.5^\circ \times 2.5^\circ$ grid. The maximum AI measurement time (local 1:30 p.m.) was used as the starting time of trajectory model. Plumes that can be tracked back to a fire region within 2 d were classified as “young”, while plumes that have been removed from their fire regions for longer than two days were defined as “aged”. We found 19 young and 4 aged plumes, which are shown in Fig. 3 as red and blue symbols, respectively. Table 1 lists the date, maximum AI and top height of each plume, its latitude and longitude of maximum AI, and age class.

Biomass burning plume heights using aerosol index measurements

H. Guan et al.

[Title Page](#)[Abstract](#)[Introduction](#)[Conclusions](#)[References](#)[Tables](#)[Figures](#)[⏪](#)[⏩](#)[◀](#)[▶](#)[Back](#)[Close](#)[Full Screen / Esc](#)[Printer-friendly Version](#)[Interactive Discussion](#)

4 Results

The inclined black line in Fig. 3 represents a minimum altitude of the top of a plume observed with a given AI value (lower bounding line):

$$\text{Minimum height (km)} = 1.2\text{AI} - 5.4 \quad (1)$$

This bounding line suggests that for all plumes, when the observed AI value is larger than 9, the plume altitude is higher than 5 km. This provides an AI threshold for identifying high-altitude injection plumes even if a direct height measurement is not available. This threshold value of AI is similar to that reported by Fromm et al. (2008b), who reported that unusually large AI values (10 or larger) were associated with smoke in the UT/LS.

While a threshold AI value is useful for categorizing high altitude plumes, there is more information that can be extracted from Fig. 3. The red line is the best-fit line to the young plumes with a corresponding equation of:

$$\text{Average height (km)} = 1.1\text{AI} - 1.2 \quad (2)$$

There was a clear tendency for young plumes to show AI values increasing with increasing altitude. This suggested that a common controlling process is operative in young biomass burning plumes. Using a radiative transfer model, Wong and Li (2002) showed that the top-of-atmosphere reflectance at channel-1 wavelength (centered around 0.65 μm) of the AVHRR sensor reached a constant level when aerosol optical depth exceeded a threshold value. We propose that most of the analyzed large-AI young plumes are sufficiently optically thick so that AI is close to or reaches an asymptote with respect to aerosol optical depth at $\sim 360\text{ nm}$, similar to the behavior suggested by Wong and Li's calculation for a longer wavelength (2002). When this occurs, and because SSA is not expected to vary a great deal (Jeong and Hsu, 2008), plume height will determine the value of AI. That is, an increasing plume height will be associated with increasing AI, as shown in Fig. 3. Figure 3 also reveals the variability of young-plume heights for a given AI value (1-sigma $\approx 1.9\text{ km}$). This variability may reflect

Biomass burning plume heights using aerosol index measurements

H. Guan et al.

Title Page

Abstract

Introduction

Conclusions

References

Tables

Figures



Back

Close

Full Screen / Esc

Printer-friendly Version

Interactive Discussion



physical differences between plumes as a consequence of CALIPSO measuring only a small portion of the plumes.

The four aged plumes (four or five days old) shown in blue in Fig. 3 indicate that at similar altitudes, aged plumes have lower AI values than young plumes. These four plumes all originated from Australian wildfires (see Table 1). Mixing with clean air, and perhaps sedimentation as the plumes aged, was likely the driving factor in reducing the optical depth, and thus, the AI. Two of the aged plumes (with heights of 14 and 15.5 km) were from a fire on 14 December 2006 (Dirken et al., 2009), while the other two plumes (18 and 19 km) were from a fire on 7 February 2009. These aged plumes were visible in the AI data for several days. Therefore we were able to record their AI values on their first observation day, shown as triangles in Fig. 4.

Assuming the plume heights do not change during aging, the four aged (blue) data points would have been inside or near the dash shaded area when they were young (1 d old), as shown by red triangles in Fig. 4. This indirectly implies that dilution processes resulting in much smaller optical depths are one of the causes for aged plumes deviating from the AI-height relationship of young plumes. This also indirectly confirms the findings of Real et al. (2007) who showed the important role of dilution/mixing processes on reducing simulated pollutant level (or concentration).

5 Finding the geographical distribution and historical number of high-altitude plumes

The knowledge of the geographical distribution and historical number of high-altitude biomass burning plumes is critical for further understanding of their associated radiative and climate effects. In this section, we use the threshold value of $AI \geq 9$ and lower bound Eq. (1) to identify plumes above 5 km and find the geographic distribution and historical number of high-altitude plumes.

The global distribution of all $AI \geq 9$ plumes during the entire data record is displayed in Fig. 5. Given the lower bounding line shown in Fig. 3, these plumes are expected to

Biomass burning plume heights using aerosol index measurements

H. Guan et al.

Title Page

Abstract

Introduction

Conclusions

References

Tables

Figures

⏪

⏩

◀

▶

Back

Close

Full Screen / Esc

Printer-friendly Version

Interactive Discussion

be at altitudes of 5 km or higher and represent the total number of observations. That is, these plumes have been counted each day they were observed. This total number is an essential parameter when estimating the influence of pollutants on the UT/LS. Sources of error include the omission of high-altitude plumes due to optical thinness and the limited temporal resolution of polar-orbiting satellites. A careful dust-screening process has helped reduce the possibility of contamination by dust plumes.

North America, Russia/Northeast Asia, and Australia are three major biomass burning source regions yielding large AI values. The number of large AI plumes from each of these three regions during the entire AI record is shown in Fig. 6. Typically, large AI plumes occur more frequently over North America (75) than over Russia/Northeast Asia (60) or Australia (28). Previous studies have suggested that Russian fires are largely lower intensity fires, burning mainly surface fuels (Conard and Ivanova, 1997; Furyaev, 1996; Wooster and Zhang, 2004), whereas in North America much higher intensity “crown” fires predominate (Conny and Slater, 2002; Wooster and Zhang, 2004). Crown fires have a larger potential to inject pollutants to higher altitudes, which is consistent with our current analysis. Although originating from a much smaller forest area, the number of Australian high-altitude plumes is also noteworthy. These occurrences mainly resulted from the bushfires in Victoria, Australia during December 2006 and around 7 February 2009. An increase in fire number, duration, and intensity in Australia has been predicted by previous researchers (Beer and Williams, 1995; Williams et al., 2001; Cary, 2002). It will be interesting to see in the coming years if this trend persists.

The large AI screening approach described here is a useful and fast tool which is easily coupled with the best-fit equation (see Eq. 2) to establish the approximate height of dense plumes. Figure 7 displays the number of plumes for several height ranges since 1978. The plumes calculated to be between 8 and 12 km accounted for ~73% of all $AI \geq 9$ plumes, while the plumes ≥ 12 km also reached a considerable number (49). Considering their heavy mass loading and long lifetime, these highest-altitude plumes may have a most important impact on the radiative budget, climate, and chemistry. Fur-

Biomass burning plume heights using aerosol index measurements

H. Guan et al.

Title Page

Abstract

Introduction

Conclusions

References

Tables

Figures



Back

Close

Full Screen / Esc

Printer-friendly Version

Interactive Discussion

ther tracing their dilution and aging using satellite data may give additional information regarding their transport and fate.

6 Conclusions

This study shows the AI data set can be used to identify high-altitude fire plumes. The derived best-fit relationship (Eq. 2) between AI and maximum plume height for young plumes (within 2 d of the fire) can provide aerosol injection heights for model applications and validation and can also provide a method for the near-real-time monitoring of high-altitude events. The direct input of satellite-derived plume heights into chemistry transport or climate models may reduce the uncertainty of fire-related pollutant transport.

For fire plumes measured with coincident OMI and CALIPSO data from June 2006–February 2009, we found the plume height is ≥ 5 km when the AI value is ≥ 9 . During the period 1978–2009, large AI (≥ 9) plumes, and therefore likely high-altitude, occurred more frequently over North America ($\sim 46\%$) than over Australia ($\sim 17\%$) or Russia/Northeast Asia ($\sim 37\%$). According to the relationship derived using coincident measurements, during this interval, 181 plumes reached altitudes above 8 km. About 73% (132) of the plumes had injection heights ≥ 8 km but below 12 km, and 49 were lofted to 12 km or higher, including fourteen plumes injected to 16 km or above.

This large AI screening approach provides a useful and fast tool to estimate the approximate height of plumes. However, this height determination approach is biased in favor of dense high-altitude smoke because of the reduced sensitivity of AI to low-altitude aerosols. Methods for detecting lower plumes and optically-thin high-altitude plumes are being explored.

Acknowledgements. The authors would like to thank the NASA/GSFC TOMS Ozone Processing Team for AI data. CALIPSO data were obtained from the NASA Langley Research Center Atmospheric Science Data Center. The authors are grateful to the MODIS science team for the production and distribution of the fire data. The authors would also like to acknowledge the

Biomass burning plume heights using aerosol index measurements

H. Guan et al.

Title Page

Abstract

Introduction

Conclusions

References

Tables

Figures

⏪

⏩

◀

▶

Back

Close

Full Screen / Esc

Printer-friendly Version

Interactive Discussion



helpful advice and commentary of Patrick Hamill. Special appreciation goes to Omar Torres, Ping Yang, and Ali Omar who provided valuable comments and suggestions for understanding AI and CALIPSO aerosol products. Funding for this work was provided by NASA's Atmospheric Composition Program (proposal number: AURA/04-0223 from NRA# NNH04ZYS004N).

5 References

- Beer, T. and Williams, A.: Estimating Australian forest fire danger under conditions of doubled carbon dioxide concentrations, *Climatic Change*, 29, 169–188, 1995.
- Cary, G. J.: Importance of a changing climate for fire regimes in Australia, in: *Flammable Australia – The Fire Regimes and Biodiversity of a Continent*, edited by: Bradstock, R. A., Gill, W. J., and William, A. M., Cambridge University Press, Cambridge, 27–46, 2002.
- Chen, Y., Li, Q., Randerson, J. T., Lyons, E. A., Kahn, R. A., Nelson, D. L., and Diner, D. J.: The sensitivity of CO and aerosol transport to the temporal and vertical distribution of North American boreal fire emissions, *Atmos. Chem. Phys.*, 9, 6559–6580, 2009, <http://www.atmos-chem-phys.net/9/6559/2009/>.
- Cofer, W. R. I., Winstead, E. L., Stocks, B. J., Overbay, L. W., Goldammer, J. G., Cahoon, D. R., and Levine, J. S.: Emissions from boreal forest fires: are the atmospheric impacts underestimated?, in: *Biomass Burning and Global Change*, edited by: Levine, J. S., MIT Press, Cambridge, Massachusetts, 1996.
- Colarco, P. R., Schoeberl, M. R., Doddridge, B. G., Marufu, L. T., Torres, O., and Welton, E. J.: Transport of smoke from Canadian forest fires to the surface near Washington, D.C.: injection height, entrainment, and optical properties, *J. Geophys. Res.*, 109, D06203, doi:10.1029/2003JD004248, 2004.
- Conard, S. G. and Ivanova, G. A.: Wildfire in Russian boreal forests – potential impacts of fire regime characteristics on emissions and global carbon balance estimates, *Environ. Pollut.*, 98, 305–313, 1997.
- Conny, J. M. and Slater, J. F.: Black carbon and organic carbon in aerosol particles from crown fires in the Canadian boreal forest, *J. Geophys. Res.*, 107(D11), 4116, doi:10.1029/2001JD001528, 2002.
- Dirksen, R. J., Boersma, K. F., de Laat, J., Stammes, P., van der Werf, G. R., Val Martin, M., and Kelder, H. M.: An aerosol boomerang: rapid around-the-world transport of smoke from the

Biomass burning plume heights using aerosol index measurements

H. Guan et al.

Title Page

Abstract

Introduction

Conclusions

References

Tables

Figures

⏪

⏩

◀

▶

Back

Close

Full Screen / Esc

Printer-friendly Version

Interactive Discussion

December 2006 Australian forest fires observed from space, *J. Geophys. Res.*, 114, D21201, doi:10.1029/2009JD012360, 2009.

Duncan, B. N., Strahan, S. E., Yoshida, Y., Steenrod, S. D., and Livesey, N.: Model study of the cross-tropopause transport of biomass burning pollution, *Atmos. Chem. Phys.*, 7, 3713–3736, 2007,

<http://www.atmos-chem-phys.net/7/3713/2007/>.

Eckhardt, S., Prata, A. J., Seibert, P., Stebel, K., and Stohl, A.: Estimation of the vertical profile of sulfur dioxide injection into the atmosphere by a volcanic eruption using satellite column measurements and inverse transport modeling, *Atmos. Chem. Phys.*, 8, 3881–3897, 2008,

<http://www.atmos-chem-phys.net/8/3881/2008/>.

Forster, C., Wandinger, U., Wotawa, G., James, P., Mattis, I., Althausen, D., Simmonds, P., O'Doherty, S., Kleefeld, C., Jennings, S. G., Schneider, J., Trickl, T., Kreipl, S., Jaeger, H., and Stohl, A.: Transport of boreal forest fire emissions from Canada to Europe, *J. Geophys. Res.*, 106(D19), 22887–22906, 2001.

Freitas, S. R., Longo, K. M., Chatfield, R., Latham, D., Silva Dias, M. A. F., Andreae, M. O., Prins, E., Santos, J. C., Gielow, R., and Carvalho Jr., J. A.: Including the sub-grid scale plume rise of vegetation fires in low resolution atmospheric transport models, *Atmos. Chem. Phys.*, 7, 3385–3398, 2007,

<http://www.atmos-chem-phys.net/7/3385/2007/>.

Fromm, M. D., Torres, O., Diner, D., et al.: Stratospheric impact of the Chisholm pyrocumulonimbus eruption: 1. Earth-viewing satellite perspective, *J. Geophys. Res.*, 113, D08202, doi:10.1029/2007JD009153, 2008a.

Fromm, M. D., Shettle, E. P., Fricke, K. H., et al.: Stratospheric impact of the Chisholm pyrocumulonimbus eruption: 2. Vertical profile perspective, *J. Geophys. Res.*, 113, D08203, doi:10.1029/2007JD009147, 2008b.

Fromm, M. D. and Servranckx, R.: Transport of forest fire smoke above the tropopause by supercell convection, *Geophys. Res. Lett.*, 30(10), 1542, doi:10.1029/2002GL016820, 2003.

Furyaev, V. V.: Pyrological regimes and dynamics of the southern taiga forests in Siberia, in: *Fire in Ecosystems of Boreal Eurasia*, edited by: Goldammer, J. G. and Furyaev, V. V., Kluwer Acad., Norwell, Mass, 168–185, 1996.

Ginoux, P., Chin, M., Tegen, I., Prospero, J. M., Holben, B., Dubovik, O., and Lin, S.-J.: Sources and distributions of dust aerosols simulated with the GOCART model, *J. Geophys. Res.*, 106(D17), 20255–20274, doi:10.1029/2000JD000053, 2001.

**Biomass burning
plume heights using
aerosol index
measurements**

H. Guan et al.

Title Page

Abstract

Introduction

Conclusions

References

Tables

Figures

◀

▶

◀

▶

Back

Close

Full Screen / Esc

Printer-friendly Version

Interactive Discussion

**Biomass burning
plume heights using
aerosol index
measurements**

H. Guan et al.

[Title Page](#)[Abstract](#)[Introduction](#)[Conclusions](#)[References](#)[Tables](#)[Figures](#)[⏪](#)[⏩](#)[◀](#)[▶](#)[Back](#)[Close](#)[Full Screen / Esc](#)[Printer-friendly Version](#)[Interactive Discussion](#)

- Guan, H., Chatfield, R. B., Freitas, S. R., Bergstrom, R. W., and Longo, K. M.: Modeling the effect of plume-rise on the transport of carbon monoxide over Africa with NCAR CAM, *Atmos. Chem. Phys.*, 8, 6801–6812, 2008, <http://www.atmos-chem-phys.net/8/6801/2008/>.
- 5 Herman, J. R., Bhartia, P. K., Torres, O., Hsu, C., Sefstor, C., and Celarier, E.: Global distribution of UV-absorbing aerosols from Nimbus 7/TOMS data, *J. Geophys. Res.*, 102(D14), 16911–16922, 1997.
- Hsu, N. C., Si-Chee, T., King, M. D., and Herman, J. R.: Aerosol properties over bright-reflecting source regions, *IEEE T. Geosci. Remote*, 42, 557–569, 2004.
- 10 IPCC: Climate Change 2007: The Physical Science Basis, Contribution of Working Group I to the Fourth Assessment Report of the Intergovernmental Panel on Climate Change, edited by: Solomon, S., Qin, D., Manning, M., Chen, Z., Marquis, M., Averyt, K. B., Tignor, M., and Miller, H. L., Cambridge University Press, Cambridge, UK and New York, NY, USA, 996 pp., 2007.
- 15 Jeong, M.-J. and Hsu, N. C.: Retrievals of aerosol single-scattering albedo and effective aerosol layer height for biomass-burning smoke: synergy derived from “A-Train” sensors, *Geophys. Res. Lett.*, 35, L24801, doi:10.1029/2008GL036279, 2008.
- Jost, H.-J., Drdla, K., Stohl, A., Pfister, L., Loewenstein, M., Lopez, J. P., Hudson, P. K., Murphy, D. M., Cziczo, D. J., Fromm, M. D., Bui, T. P., Dean-Day, J., Gerbig, C., Mahoney, M. J., Richard, E. C., Spichtinger, N., Pittman Vellovic, J., Weinstock, E. M., Wilson, J. C., and Xueref, I.: In-situ observations of mid-latitude forest fire plumes deep in the stratosphere, *Geophys. Res. Lett.*, 31, L11101, doi:10.1029/2003GL019253, 2004.
- 20 Kahn, R. A., Chen, Y., Nelson, D. L., Leung, F.-Y., Li, Q., Diner, D. J., and Logan, J. A.: Wildfire smoke injection heights: Two perspectives from space, *Geophys. Res. Lett.*, 35, L04809, doi:10.1029/2007GL032165, 2008.
- Kiss, P., Janosi, I. M., and Torres, O.: Early calibration problems detected in TOMS Earth-Probe aerosol signal, *Geophys. Res. Lett.*, 34, L07803, doi:10.1029/2006GL028108, 2007.
- Kuester, M. A., Marshall, J., and Emery, W. J.: Remote sensing and modeling of wildfires, *Proceedings of the Geoscience and Remote Sensing Symposium, 2005, IGARSS '05, IEEE International*, 5729–5732, 2005.
- 30 Li, Q., Jiang, J. H., Wu, D. L., Read, W. G., Livesey, N. J., Waters, J. W., Zhang, Y., Wang, B., Filipiak, M. J., Davis, C. P., Turquety, S., Wu, S., Park, R. J., Yantosca, R. M., and Jacob, D. J.: Convective outflow of South Asian pollution: a global CTM simulation compared with EOS

**Biomass burning
plume heights using
aerosol index
measurements**

H. Guan et al.

Title Page

Abstract

Introduction

Conclusions

References

Tables

Figures

◀

▶

◀

▶

Back

Close

Full Screen / Esc

Printer-friendly Version

Interactive Discussion

- MLS observations, *Geophys. Res. Lett.*, 32, L14826, doi:10.1029/2005GL022762, 2005.
- Luderer, G., Trentmann, J., Winterrath, T., Textor, C., Herzog, M., Graf, H. F., and Andreae, M. O.: Modeling of biomass smoke injection into the lower stratosphere by a large forest fire (Part II): sensitivity studies, *Atmos. Chem. Phys.*, 6, 5261–5277, 2006, <http://www.atmos-chem-phys.net/6/5261/2006/>.
- Mazzoni, D., Logan, J. A., Diner, D., Kahn, R., Tong, L., and Li, Q.: A data-mining approach to associating MISR smoke plume heights with MODIS fire measurements, *Remote Sens. Environ.*, 107, 149–158, doi:10.1016/j.rse.2006.08.014, 2007.
- Randerson, J. T., Liu, H., Flanner, M. G., Chambers, S. D., Jin, Y., Hess, P. G., Pfister, G., Mack, M. C., Treseder, K. K., Welp, L. R., Chapin, F. S., Harden, J. W., Goulden, M. L., Lyons, E., Neff, J. C., Schuur, E. A. G., and Zender, C. S.: The impact of boreal forest fire on climate warming, *Science*, 314, 1130–1132, doi:10.1126/science.1132075, 2006.
- Real, E., Law, K. S., Weinzierl, B., et al.: Processes influencing ozone levels in Alaskan forest fire plumes during long-range transport over the North Atlantic, *J. Geophys. Res.*, 112, D10S41, doi:10.1029/2006JD007576, 2007.
- Rosenfeld, D., Fromm, M., Trentmann, J., Luderer, G., Andreae, M. O., and Servranckx, R.: The Chisholm firestorm: observed microstructure, precipitation and lightning activity of a pyro-cumulonimbus, *Atmos. Chem. Phys.*, 7, 645–659, 2007, <http://www.atmos-chem-phys.net/7/645/2007/>.
- Schoeberl, M. and Newman, P. A.: A multiple-level trajectory analysis of vortex filaments, *J. Geophys. Res.*, 100(D12), 25801–25815, 1995.
- Thomason, L. W., Pitts, M. C., and Winker, D. M.: CALIPSO observations of stratospheric aerosols: a preliminary assessment, *Atmos. Chem. Phys.*, 7, 5283–5290, 2007, <http://www.atmos-chem-phys.net/7/5283/2007/>.
- Torres, O., Bhartia, P. K., Herman, J. R., Ahmad, Z., and Gleason, J.: Derivation of aerosol properties from satellite measurements of backscattered ultraviolet radiation: theoretical basis, *J. Geophys. Res.*, 103, 17099–17110, doi:10.1029/98JD00900, 1998.
- Torres, O., Tanskanen, A., Veihelmann, B., Ahn, C., Braak, R., Bhartia, P. K., Veefkind, P., and Levelt, P.: Aerosols and surface UV products from Ozone Monitoring Instrument observations: an overview, *J. Geophys. Res.*, 112, D24S47, doi:10.1029/2007JD008809, 2007.
- Trentmann, J., Luderer, G., Winterrath, T., Fromm, M. D., Servranckx, R., Textor, C., Herzog, M., Graf, H.-F., and Andreae, M. O.: Modeling of biomass smoke injection into the lower stratosphere by a large forest fire (Part I): reference simulation, *Atmos. Chem. Phys.*, 6,

5247–5260, 2006,

<http://www.atmos-chem-phys.net/6/5247/2006/>.

Val Martin, M., Logan, J. A., Kahn, D., Leung, F. Y., Nelson, D., and Diner, D.: Smoke injection heights from fires in North America: analysis of 5 years of satellite observations, *Atmos.*

Chem. Phys. Discuss., 9, 20515–20566, 2009,

<http://www.atmos-chem-phys-discuss.net/9/20515/2009/>.

Vaughan, M., Young, S., Winker, D., Powell, K., Omar, A., Liu, Z., Hu, Y., and Hosteler, C.: Fully automated analysis of space-based lidar data: an overview of CALIPSO retrieval algorithms and data products, *Proc. SPIE*, 5575, 16–30, 2004.

Waibel, A. E., Fischer, H., Wienhold, F. G., Siegmund, P. C., Lee, B., Strom, J., Lelieveld, J., and Crutzen, P. J.: Highly elevated carbon monoxide concentrations in the upper troposphere and lowermost stratosphere at northern midlatitudes during the STREAM II summer campaign in 1994, *Chemosphere*, 1, 233–248, 1999.

Westphal, D. L. and Toon, O. B.: Simulations of microphysical, radiative, and dynamical processes in a continental-scale forest fire smoke plume, *J. Geophys. Res.*, 96(D12), 22379–22400, doi:10.1029/91JD01956, 1991.

Williams, A. A. J., Karoly, D. J., and Tapper, N.: The sensitivity of Australian fire danger to climate change, *Climatic Change*, 49, 171–191, 2001.

Winker, D. M., Hunt, W. H., and McGill, M. J.: Initial performance assessment of CALIOP, *Geophys. Res. Lett.*, 34, L19803, doi:10.1029/2007GL030135, 2007.

Wong, J. and Li, Z.: Retrieval of optical depth for heavy smoke aerosol plumes: uncertainties and sensitivities to the optical properties, *J. Atmos. Sci.*, 59, 250–261, 2002.

Wooster, M. J. and Zhang, Y. H.: Boreal forest fires burn less intensely in Russia than in North America, *Geophys. Res. Lett.*, 31, L20505, doi:10.1029/2004GL020805, 2004.

**Biomass burning
plume heights using
aerosol index
measurements**

H. Guan et al.

Title Page

Abstract

Introduction

Conclusions

References

Tables

Figures

⏪

⏩

◀

▶

Back

Close

Full Screen / Esc

Printer-friendly Version

Interactive Discussion

Table 1. The dates of large-AI biomass burning plumes with coincident CALIPSO data.

Date	Plume height (km)	Maximum AI	Lat.	Lon.	Age class ^a
24 Jul 06	4.5	8.2	62.5	103.5	Y
25 Jul 06	10.6	9.2	63.5	100.5	Y
26 Jul 06	12.0	14.6	61.5	110.5	Y
27 Jul 06	12.6	11.1	64.5	114.5	Y
27 Jul 06	7.5	7.8	72.5	97.5	Y
5 Sep 06	12.3	11.4	48.5	-89.5	Y
5 Sep 06	9.9	8.6	47.5	-109.5	Y
19 Dec 06	15.6	9.3	-37.5	-78.5	A
19 Dec 06	14.0	7.6	-39.5	-69.5	A
26 May 07	7.5	8.1	47.5	-63.5	Y
10 Jun 07	15.6	15.4	39.5	122.5	Y
8 Jul 07	12.0	7.9	33.5	-104.5	Y
30 Jul 07	8.7	10.1	49.5	-103.5	Y
1 Aug 07	6.0	7.2	47.5	-94.5	Y
1 Aug 07	4.5	7.1	-8.5	11.5	Y
13 Aug 07	4.8	8.6	47.5	-109.5	Y
14 Aug 07	7.5	8.8	45.5	-89.5	Y
15 Aug 07	6.0	7.0	44.5	-98.5	Y
17 Aug 07	7.0	7.2	43.5	-99.5	Y
2 Jul 08	7.0	7.3	53.5	147.5	Y
9 Feb 09	13.8	12.4	-24.5	-175.5	Y
11 Feb 09	17.8	7.0	-32.5	-169.5	A
12 Feb 09	19.0	7.1	-30.5	-175.5	A

^a Y=Young (<2 d old) and A=Aged (>2 d old)

Biomass burning plume heights using aerosol index measurements

H. Guan et al.

Title Page

Abstract

Introduction

Conclusions

References

Tables

Figures

◀

▶

◀

▶

Back

Close

Full Screen / Esc

Printer-friendly Version

Interactive Discussion



**Biomass burning
plume heights using
aerosol index
measurements**

H. Guan et al.

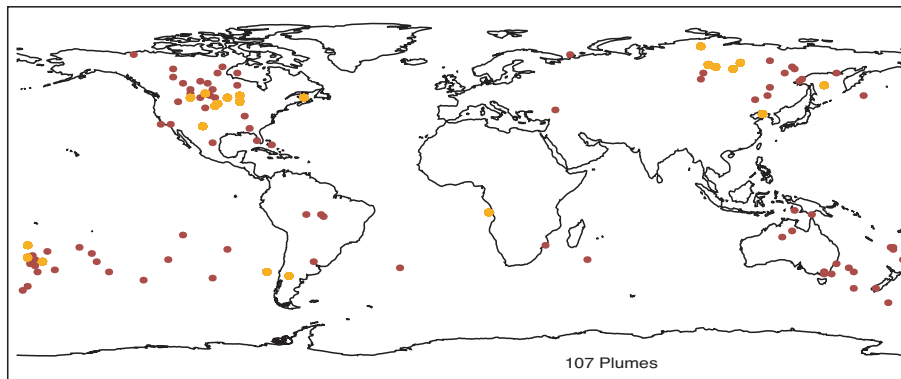
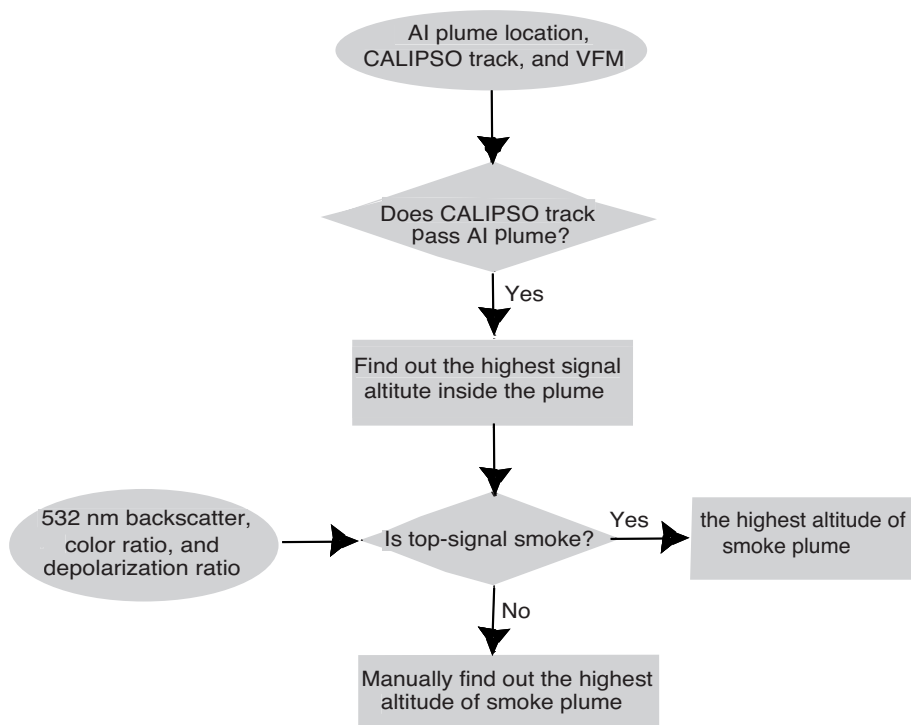


Fig. 1. Locations of AI plumes encountered during the CALIPSO era (1 June 2006 to 13 February 2009). An aerosol plume is defined as containing at least 1 pixel with $AI \geq 7$ and at least 3 adjacent pixels with $AI \geq 4$. Orange symbols represent the cases of coincident AI and CALIPSO measurements.

[Title Page](#)[Abstract](#)[Introduction](#)[Conclusions](#)[References](#)[Tables](#)[Figures](#)[⏪](#)[⏩](#)[◀](#)[▶](#)[Back](#)[Close](#)[Full Screen / Esc](#)[Printer-friendly Version](#)[Interactive Discussion](#)

**Biomass burning
plume heights using
aerosol index
measurements**

H. Guan et al.

**Fig. 2.** Flowchart for the determination of highest plume altitude along the CALIPSO track.[Title Page](#)[Abstract](#)[Introduction](#)[Conclusions](#)[References](#)[Tables](#)[Figures](#)[⏪](#)[⏩](#)[◀](#)[▶](#)[Back](#)[Close](#)[Full Screen / Esc](#)[Printer-friendly Version](#)[Interactive Discussion](#)

**Biomass burning
plume heights using
aerosol index
measurements**

H. Guan et al.

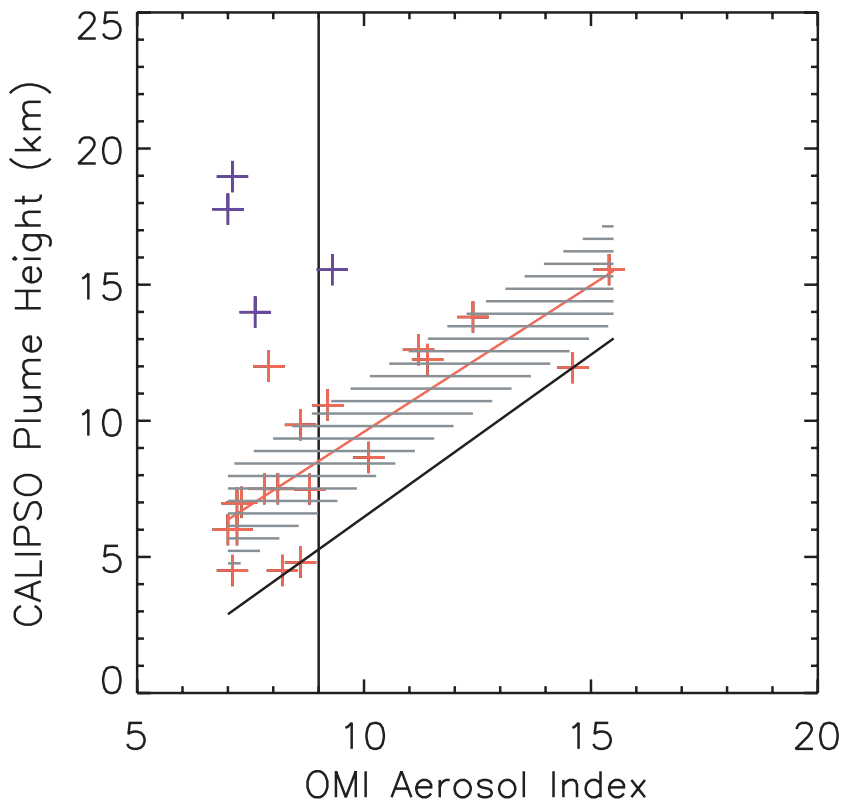


Fig. 3. Scatter-plot of OMI AI and CALIPSO maximum plume height. Red and blue symbols represent “young” and “aged” plumes, respectively. The inclined black line ($Z=1.2AI-5.4$) is the lower bound to the young plume data. The black vertical line indicates an AI threshold ($AI=9$) for high-altitude (≥ 5 km) plumes. The red line ($Z=1.1AI-1.2$) is the best fit to the young plumes. The shaded area shows a ± 1 standard deviation ($1-\sigma \approx 1.9$ km) across the best fit of the young plumes.

[Title Page](#)[Abstract](#)[Introduction](#)[Conclusions](#)[References](#)[Tables](#)[Figures](#)[◀](#)[▶](#)[◀](#)[▶](#)[Back](#)[Close](#)[Full Screen / Esc](#)[Printer-friendly Version](#)[Interactive Discussion](#)

**Biomass burning
plume heights using
aerosol index
measurements**

H. Guan et al.

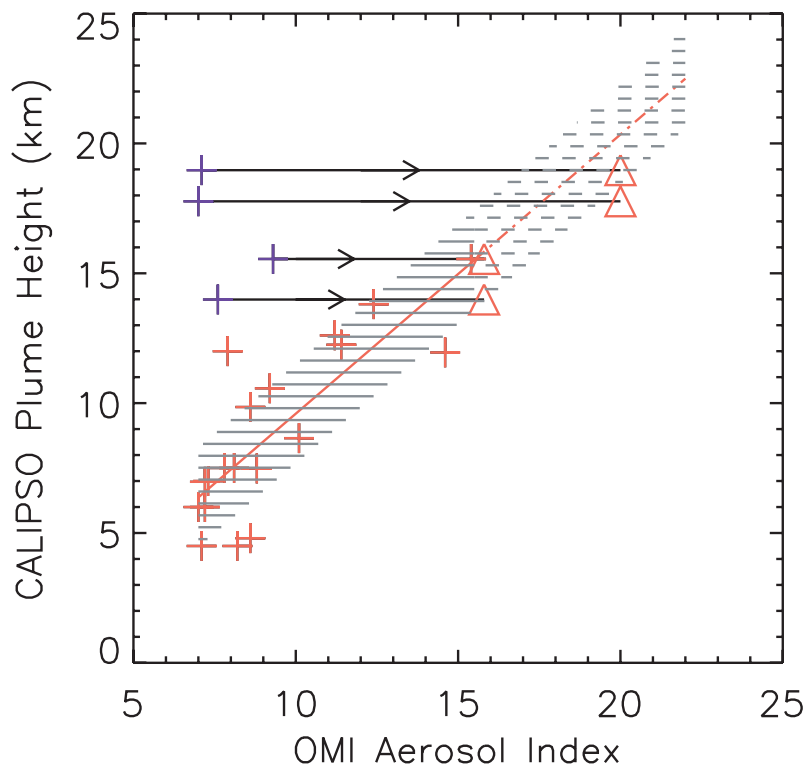


Fig. 4. Scatter-plot of OMI AI and CALIPSO maximum plume height. Red and blue symbols represent “young” and “aged” plumes, respectively, as described in Fig. 3. Solid shaded area shows ± 1 standard deviation ($1-\sigma \approx 1.9$ km) across the best fit of the young plumes. Assuming the height is not changed during transport, the 4 aged plumes (blue data points) would have been inside or near the shaded area when they were young (red triangles), based on OMI observations 3 or 4 d before the observations shown as blue crosses. No coincident CALIPSO data were available to confirm this assumption.

[Title Page](#)[Abstract](#)[Introduction](#)[Conclusions](#)[References](#)[Tables](#)[Figures](#)[◀](#)[▶](#)[◀](#)[▶](#)[Back](#)[Close](#)[Full Screen / Esc](#)[Printer-friendly Version](#)[Interactive Discussion](#)

**Biomass burning
plume heights using
aerosol index
measurements**

H. Guan et al.

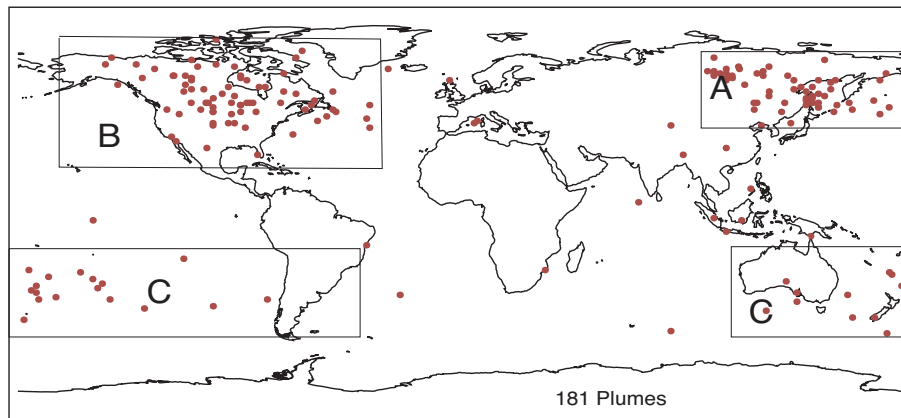


Fig. 5. Global distribution of high-altitude plumes with an AI value ≥ 9 (i.e. height ≥ 5 km) during the entire AI data record (31 October 1978 to 13 February 2009). 181 plumes were identified, and 163 of those are located in three main regions.

[Title Page](#)[Abstract](#)[Introduction](#)[Conclusions](#)[References](#)[Tables](#)[Figures](#)[◀](#)[▶](#)[◀](#)[▶](#)[Back](#)[Close](#)[Full Screen / Esc](#)[Printer-friendly Version](#)[Interactive Discussion](#)

**Biomass burning
plume heights using
aerosol index
measurements**

H. Guan et al.

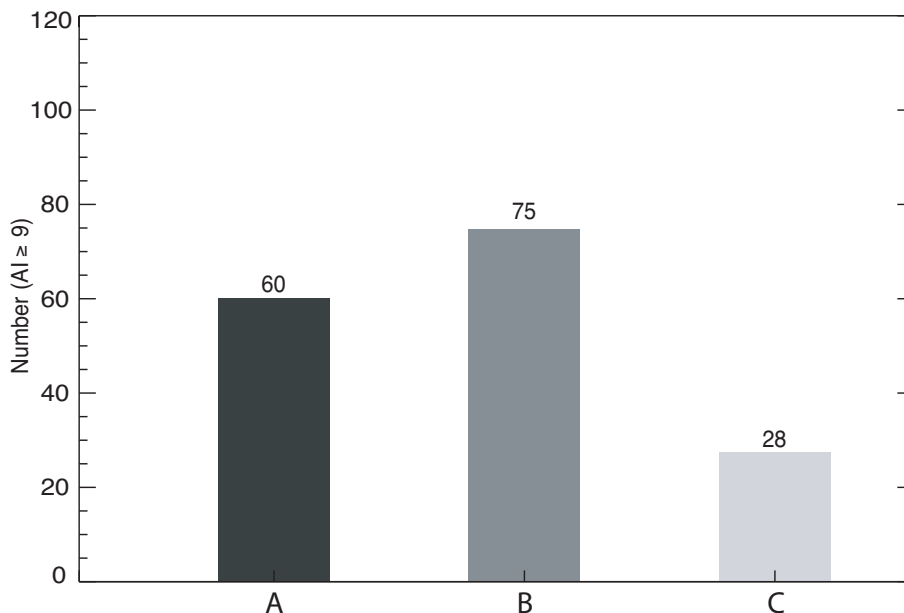


Fig. 6. Number of large-AI (≥ 9) observations over the three regions shown in Fig. 5 during the entire AI data record. Region A represents plumes over Russia and North Asia, B is North America, and C includes plumes over and downwind of Australia.

[Title Page](#)[Abstract](#)[Introduction](#)[Conclusions](#)[References](#)[Tables](#)[Figures](#)[⏪](#)[⏩](#)[◀](#)[▶](#)[Back](#)[Close](#)[Full Screen / Esc](#)[Printer-friendly Version](#)[Interactive Discussion](#)

**Biomass burning
plume heights using
aerosol index
measurements**

H. Guan et al.

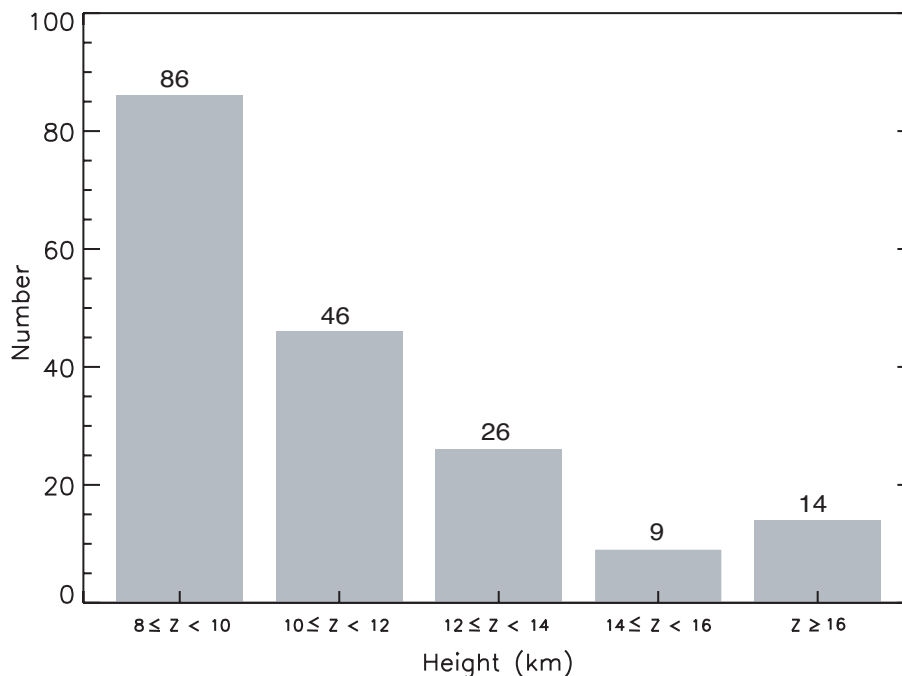


Fig. 7. Number of plumes for each height range during the entire AI data record (31 October 1978 to 13 February 2009). Heights are calculated using the equation of the best-fit (red) line in Fig. 3.

[Title Page](#)[Abstract](#)[Introduction](#)[Conclusions](#)[References](#)[Tables](#)[Figures](#)[◀](#)[▶](#)[◀](#)[▶](#)[Back](#)[Close](#)[Full Screen / Esc](#)[Printer-friendly Version](#)[Interactive Discussion](#)